Macromolecules
A R T I C L E

Micelle Formation in Block Copolymer/Homopolymer Blends: Comparison of Self-Consistent Field Theory with Experiment and Scaling Theory

Martin J. Greenall,[*,†] **D. Martin A. Buzza,**[‡] **and Thomas C. B. McLeish**[†,§]

[†]*School of Physics and Astronomy, University of Leeds, Leeds LS2 9JT, U.K., and* [‡]*Department of Physics, The University of Hull, Cottingham Road, Hull HU6 7RX, U.K.* [§]*Present address: Department of Physics, Durham University, South Road, Durham DH1 3LE, U.K.*

ABSTRACT: We present a self-consistent field theory (SCFT) study of spherical micelle formation in a blend of poly(styrene−butadiene) diblocks and homopolystyrene. The micelle core radii, corona thicknesses, and critical micelle concentrations are calculated as functions of the polymer molecular weights and the composition of the diblocks. We then make a parameter-free comparison of our results with an earlier scaling theory and X-ray scattering data. For the micelle core radii R_c, we find that SCFT reproduces the shape of the variation of R_c with different molecular parameters much more accurately compared to scaling theory, though, like scaling theory, it overestimates R_c by about 20−30%. For the corona thickness L_c, the accuracy of our SCFT results is at least as good as that of scaling theory. For copolymers with lighter core blocks, SCFT predictions for the critical micelle concentration improve over those of scaling theories by an order of magnitude. In the case of heavier core blocks, however, SCFT predicts the critical micelle concentration less well due to inaccuracies in the modeling of the bulk chemical potential. Overall, we find that SCFT gives a good description of spherical micelle formation and is generally more successful than scaling theory.

1. Introduction

When dissolved in a solvent such as water, amphiphilic block copolymers can self-assemble into micelles similar to those seen in low molecular weight surfactants.[1] The solvophobic blocks cluster together to form a core, and the solvophilic blocks spread outward as a corona. A certain minimum concentration is needed for micelles to form: this is the critical micelle concentration, or cmc.[2] These block copolymer micelles have been the subject of growing recent interest, from the points of view of both fundamental polymer physics[3] and potential applications, particularly in drug delivery.[4]

A closely related system, which is the subject of this paper, is a blend of block copolymer and homopolymer. Here, the block copolymers may also form micelles, with the homopolymer acting as the solvent.[5,6] This system is more easily controlled and better characterized than an aqueous solution of diblocks and so is more suitable for a study of the fundamentals of micelle formation. In particular, the interaction strengths between the different components are well described by the standard χ parameter[7] and can be obtained from the literature.[8]

Detailed experimental data are available on spherical micelle formation in these blends.[5,9,10] These data have been modeled using scaling theories.[5,6,11−13] However, while qualitatively reproducing the general trends seen in these systems (for example, the increase in the micelle core radius as the homopolymer length is increased), scaling often fails to predict the shape or magnitude of these variations quantitatively. In this paper, we use a more microscopic approach which involves less severe approximations: self-consistent field theory (SCFT).[7,14] SCFT, a mean-field theory of an ensemble of flexible polymers, is probably the most successful theoretical method for the modeling of the structures

formed by polymers and provides quantitative results on polymer melts.[7] To our knowledge, the properties of micelles in copolymer/homopolymer blends have not been studied in detail, using experimentally determined polymer properties, with SCFT. Although a considerable body of work exists on the self-consistent field theory of micelle formation, this mostly focuses on diblocks dispersed in monomer solvent[15−17] or on diblock copolymer melts[18] (although see the paper by Duque on intermediate states in micelle formation[19] and that by Monzen et al.[20] on triblocks in homopolymer). A further motivation for the study of micelles using SCFT is that much previous research using this approach has concentrated on periodic structures.[7] In contrast to this, our work is a detailed test of the theory for isolated aggregates and provides an assessment of the suitability of SCFT for the investigation of the self-assembly of polymers in solution and the design of macromolecules for applications.

We focus on the X-ray scattering experiments of Kinning, Thomas, and Fetters,[5] which study poly(styrene−butadiene) diblocks in homopolystyrene. We compare our predictions with their results on the core and corona radii and the critical micelle concentration. Our SCFT results are also compared with the scaling theory predictions of Leibler, Orland, Wheeler, and others.[6,11−13]

2. Details of System and Scaling Theory

Kinning, Thomas, and Fetters[5] studied blends of poly-(styrene−butadiene) diblock copolymer and polystyrene homopolymer. In order to determine the effects of the molecular weight of the polymers and the relative amounts of styrene and butadiene in the diblocks, several samples were considered. We adopt the notation used by these authors[5] to label the samples. As an example, a diblock sample of polystyrene molar weight 60 kg/mol and polybutadiene molar weight 10 kg/mol is referred to as SB

*Corresponding author. E-mail: m.j.greenall@leeds.ac.uk

60/10. A polystyrene homopolymer sample of molar weight 2.1 kg/mol is labeled 2100 PS. Note that these values are quite rough: more precise molecular weights for the individual samples are tabulated in the original paper.[5]

The polymer samples are characterized by their specific volumes, the root-mean-square end-to-end distances of the polymer molecules, and the polystyrene–polybutadiene interaction energy density. We now introduce and discuss these quantities.

The specific volume of PB as a function of temperature is given empirically by[8]

$$V_{PB} \ (cm^3/g) \approx 1.0968 + (8.24 \times 10^{-4})T \quad (1)$$

while that of PS has been found[21] to be

$$V_{PS} \ (cm^3/g) \approx 0.9217 + (5.412 \times 10^{-4})T + (1.678 \times 10^{-7})T^2 \quad (2)$$

The temperature T is measured in degrees Celsius and is equal to 115 °C in all experiments considered here.

SCFT is more naturally written in terms of the volumes of individual molecules v_i, with i representing either PB or PS. These can be calculated from eqs 1 and 2 by[5]

$$v_i \ (\mathring{A}^3) = M_i \ (g/mol) \times V_i \ (cm^3/g)/0.602 \quad (3)$$

where M_i is the molar weight of substance i.

The polymer root-mean-square end-to-end distances are given, also empirically, by[5]

$$\langle R_{PB}^2 \rangle^{1/2} \ (\mathring{A}) \approx 0.93 M_{PB}^{1/2}$$
$$\langle R_{PS}^2 \rangle^{1/2} \ (\mathring{A}) \approx 0.70 M_{PS}^{1/2} \quad (4)$$

where the molecular weights are measured in g/mol. The work of Kinning et al. differs from much of the polymer literature in that it characterizes the strength of the interaction between the two polymer species via the interaction energy density Λ,[6] rather than the corresponding χ parameter. The energy of this interaction is given by

$$\Lambda \int d\mathbf{r} \ \phi_{PS}(\mathbf{r}) \ \phi_{PB}(\mathbf{r}) \quad (5)$$

where the $\phi_i(\mathbf{r})$ terms are the local volume fractions of the two polymer species at position $\mathbf{r}$. The definition of the χ parameter involves the introduction of an arbitrary reference volume V_{ref}, such as the average of the repeat unit volumes of the two polymers.[7] However, it is always possible to write terms involving the interaction strength in such a way that the numerical value of V_{ref} need not be specified. Thus, Λ, which requires no reference volume, is preferred by some authors. For reference, χ and Λ are related by[6]

$$\Lambda = \chi (V_{ref}/k_B T)^{-1} \quad (6)$$

where k_B is Boltzmann's constant.

Data on the temperature dependence of the polystyrene–polybutadiene interaction energy density may be fitted by the empirical formula[22]

$$\Lambda \ (cal/cm^3) = A - B(T - 150 \ °C) \quad (7)$$

where $A = 0.718 \pm 0.051$ and $B = 0.0021 \pm 0.00045$.

The parameters described here (molecular volumes, end-to-end distances, and interaction energy density) are the required input for our SCFT calculations. They are all determined from experiments that do not involve micelle formation—it is not necessary for any parameters specific to micellization to be measured in order to predict the structure of micelles.

To our knowledge, the only approach that has previously been used to provide detailed, system-specific predictions of micelle structure in copolymer/homopolymer blends is scaling theory. In the paper of Kinning et al. discussed above, the experimental data are compared with a scaling approach developed by Leibler and others.[6,11–13] Like SCFT, this theory predicts the micelle properties from the system parameters introduced above. Since scaling theory will be compared with our SCFT calculations later in this paper, we outline it briefly now.

Scaling theory assumes that the micelle consists of two distinct and uniform regions: the core and the corona, which in turn are completely distinct from the surrounding solution. The core is taken to contain B-type (solvophobic) monomers mixed with A homopolymer. Similarly, the corona is assumed to be composed of A-type monomers (belonging to the copolymer molecules) mixed with A homopolymer. The surroudings of the micelle are modeled as a homogeneous solution of homopolymer and copolymer chains. Making these clear divisions between the different regions of the micelle and the surrounding polymer solution allows the free energy of a blend containing N_m micelles to be written as

$$F_M = N_m F + F_{mix} - TS_m \quad (8)$$

where F is the free energy of a single micelle, F_{mix} is the free energy of mixing of the homopolymers and diblocks *outside* the micelles, and S_m is the translational entropy of the gas of micelles. F_{mix} is calculated from the standard Flory–Huggins expression.[23] The translational entropy S_m is calculated from a lattice model[11,13] where each lattice cell has the volume of a single micelle.[13] The number of occupied cells is calculated from the fraction of copolymer chains that aggregate into micelles.

The free energy of a single micelle F can then be split into separate contributions as follows:

$$F = 4\pi R_c^2 \gamma + F_d + F_{mA} + F_{mB} \quad (9)$$

Here, R_c is the radius of the core and γ is the interfacial tension at the core–corona boundary. The use of this expression for the interfacial energy assumes that the interface has the same properties as the interface between two incompatible homopolymers and allows γ to be simply expressed in terms of the monomer length and the χ parameter.[11]

The deformation energy F_d arises from the stretching of the copolymer chains confined to the spherical micelle. Finally, F_{mA} and F_{mB} are the free energies of mixing of the homopolymer with the copolymer blocks in the corona and core regions, respectively. Like the bulk mixing term F_{mix} in eq 8, these are assumed to be given by the Flory–Huggins theory of polymer blends.[23]

To find the equilibrium state of the system, eq 8 is minimized, keeping the temperature and total volume fraction of copolymer fixed and allowing all other quantities (such as the size and number of micelles) to vary. This yields predictions for the core and corona radii, the critical micelle concentration, and the composition of the various regions. In this paper, we compare our SCFT results with the scaling predictions of Kinning et al.[5]

3. Self-Consistent Field Theory

Self-consistent field theory (SCFT)[14] predicts the equilibrium structures formed in a melt or blend of polymers. It is a mean-field

theory, neglecting composition fluctuations. The description of the polymers is coarse-grained: the configuration of an individual polymer molecule is modeled as a random walk in space $\mathbf{r}_\alpha(s)$, where s is a curve parameter specifying the position along the polymer backbone. An ensemble of many such polymers is considered. The interactions between polymers are included in two ways: by assuming that the blend is incompressible and introducing a contact potential between molecules of different species. The strength of this potential is specified by the interaction energy density Λ.

The first step in finding an approximation method (SCFT) for the above system is to view each molecule as being acted on by a field produced by all other molecules in the system.[7] This transforms the N-body problem of modeling an ensemble of N polymers into N 1-body problems. Since we wish to compute the partition sum over all possible system configurations, all molecules of a given species may be treated as equivalent. Therefore, we need only introduce one field $W_i(\mathbf{r})$ for each species i and have only to solve i 1-body problems. Note that this involves no approximation—the complexity of the system is hidden in the field terms $W_i(\mathbf{r})$. The utility of the SCFT approach lies in the fact that approximations may be found more easily for the fields than for the original formulation of the problem.

For definiteness, we now focus on our diblock copolymer/homopolymer blend and introduce fields W_{PS}, W_{PB}, and W_{hPS} acting on the polystyrene blocks, polybutadiene blocks, and homopolystyrene, respectively. This converts the partition sum into an integral over field configurations, with the original Hamiltonian replaced by an effective Hamiltonian H. Following the procedure described in the recent review by Matsen,[7] we find that H is given by

$$\frac{H}{k_B T} = \frac{\Lambda}{k_B T} \int d\mathbf{r}\, [\Phi_{PS}(\mathbf{r}) + \Phi_{hPS}(\mathbf{r})][1 - \Phi_{PS}(\mathbf{r}) + \Phi_{hPS}(\mathbf{r})]$$
$$- \frac{1}{\nu_{PS} + \nu_{PB}} \int d\mathbf{r}\, \{W_{PS}(\mathbf{r})\Phi_{PS}(\mathbf{r}) + W_{PB}(\mathbf{r})[1 - \Phi_{PS}(\mathbf{r})$$
$$+ \Phi_{hPS}(\mathbf{r})]\} - \frac{1}{\nu_{hPS}} \int d\mathbf{r}\, W_{hPS}(\mathbf{r})\Phi_{hPS}(\mathbf{r})$$
$$- \frac{\overline{\phi}_{hPS} V}{\nu_{hPS}} \ln Q_{hPS} - \frac{(\overline{\phi}_{PS} + \overline{\phi}_{PB}) V}{\nu_{PS} + \nu_{PB}} \ln Q_{PS,PB} \quad (10)$$

where the $\Phi_i(\mathbf{r})$ are the local volume fractions of the various polymer species i (i = PS, PB, or hPS) and V is the total volume of the system. The terms $\overline{\phi}_i$ are the mean volume fractions of species i. The first term (with prefactor $\Lambda/k_B T$) describes the interaction between the different polymer species. In this term, and throughout, the polybutadiene block volume fraction $\Phi_{PB}(\mathbf{r})$ is replaced by $1 - \Phi_{PS}(\mathbf{r}) - \Phi_{hPS}(\mathbf{r})$. This follows from the incompressibility of the blend: the local volume fractions must add to 1 at every point. The next three terms all involve the $W_i(\mathbf{r})$ and arise from the unit operators that are inserted into the partition function to convert the partition sum into an integral over fields. In the penultimate term, Q_{hPS} is the partition function of a single homopolymer chain in the field $W_{hPS}(r)$. Similarly, $Q_{PS,PB}$ is the partition function of a single copolymer chain in the fields $W_{PS}(r)$ and $W_{PB}(r)$. These are given by (again following the review referenced above[7])

$$Q_{hPS}[W_{hPS}] = \int d\mathbf{r}\, q^\dagger_{hPS}(\mathbf{r}, s) q_{hPS}(\mathbf{r}, s) \quad (11)$$

where the q and $q^\dagger$ terms are single chain propagators.[7] The partition function $Q_{PS,PB}$ of a single copolymer chain is determined similarly. Recall that the polymer molecules are modeled as random walks subject to an external field that incorporates

their interactions with the rest of the melt. This is reflected in the fact that the propagators satisfy modified diffusion equations. In the case of the homopolymer, we have

$$\frac{\partial}{\partial s} q_{hPS}(\mathbf{r}, s) = \left[\frac{1}{6}\langle R_{hPS}^2 \rangle \nabla^2 - W_{hPS}(\mathbf{r})\right] q_{hPS}(\mathbf{r}, s) \quad (12)$$

with initial condition $q_{hPS}(\mathbf{r},0) = 1$. The copolymer propagators are computed in a similar way, with the copolymer architecture entering into the theory through the fact that the corresponding diffusion equation for the copolymer is solved with the field $W_i(\mathbf{r})$ and the prefactor of the $\nabla^2 q$ term appropriate to each of the two sections of the copolymer.[24]

All steps until now have been exact, and we now introduce the main approximation of SCFT. This consists of extremizing H with respect to all fields $W_i(\mathbf{r})$ and all densities $\Phi_i(\mathbf{r})$, yielding a saddle-point approximation to the system partition function Z. If the polymers are long and fluctuations are weak, this method successfully isolates the dominant contribution to Z, and the predictions of SCFT are in good agreement with experiment.[25]

Extremizing F produces a set of simultaneous equations linking the values of the fields and densities at the minimum. Denoting these values by lower-case letters $\phi_i(\mathbf{r})$ and $w_i(\mathbf{r})$, we find

$$1 = \phi_{PS}(\mathbf{r}) + \phi_{PB}(\mathbf{r}) + \phi_{hPS}(\mathbf{r})$$

$$\frac{1}{\nu_{PS} + \nu_{PB}}[w_{PS}(\mathbf{r}) - \omega_{PB}(\mathbf{r})] = \frac{2\Lambda}{k_B T}[\overline{\phi}_{PS} + \overline{\phi}_{hPS} - \phi_{PS}(\mathbf{r}) - \phi_{hps}(\mathbf{r})]$$

$$w_{hPS} = \frac{\nu_{hPS}}{\nu_{PS} + \nu_{PB}} w_{PS}(\mathbf{r}) \quad (13)$$

where $\overline{\phi}_i$ is the (mean) volume fraction of species i. The first of these equations arises directly from the incompressibility of the melt. The homopolymer density is evaluated from the propagators (see eq 12) according to[7]

$$\phi_{hPS}(\mathbf{r}) = \frac{V \overline{\phi}_{hPS}}{Q_{hPS}[w_{hPS}]} \int_0^1 ds\, q_{hPS}(\mathbf{r}, s) q^\dagger_{hPS}(\mathbf{r}, s) \quad (14)$$

The copolymer densities are calculated similarly, with the integration limits set to give the correct proportions of each species.

In order to calculate the SCFT density profiles for a given set of mean volume fractions, the set of simultaneous eqs 13 must be solved with the densities calculated as in eq 14. This is achieved using a standard relaxation procedure.[26] To begin, we make a guess for the form of the fields $w_i(\mathbf{r})$ and solve the diffusion equations to calculate the propagators and hence the densities corresponding to these fields (see eqs 12 and 14). New values for the fields are now calculated using the new $\phi_i(\mathbf{r})$. However, if we then recalculate the densities with these new w_i, we find that the relaxation algorithm becomes unstable. To avoid this problem, we (heavily) damp the iteration, replacing the $w_i(\mathbf{r})$ with a mixture of the old and new values ($0.99 w_i^{old} + 0.01 w_i^{new}$)), and then calculate the ϕ_i. The procedure is repeated until the difference between the left- and right-hand sides of eqs 13 is less than 10^{-5}. For several systems, we have confirmed that the iteration converges to the same solution for different initial guesses for the w_i.

Since we focus on isolated spherical micelles, the diffusion equations themselves are solved in a spherically symmetric geometry. Reflecting boundary conditions are imposed at the origin and at the boundary of the system. A finite difference method[27] is used to generate approximate numerical solutions to the diffusion equations. The calculations are performed in real space, in contrast to much of the SCFT literature.[28] A step size of $r = 4$ Å is used. It has been checked that using a finer grid does not significantly change the $\phi_i(\mathbf{r})$.

In the above discussion, we considered a simple system of fixed volume and fixed copolymer volume fraction containing one micelle. To find the micelle with the lowest free energy, we must consider how a system of many micelles minimizes its free energy. Consider a macroscopic copolymer/homopolymer blend whose copolymer volume fraction $\bar{\phi}_{PB} + \bar{\phi}_{PS}$, total volume V_T, and temperature T are all fixed. The equilibrium state of this system can be found by minimizing the total free energy F. If the copolymer concentration is above a certain value (the critical micelle concentration), copolymer chains can exist either as monomers or in micelles. The number density of micelles is thus an internal degree of freedom, and the macroscopic system varies this quantity (subject to the constraint of fixed copolymer volume fraction) in order to minimize the free energy.

Explicit calculations on this many-micelle macroscopic system are extremely time-consuming even using SCFT. However, we can reduce the problem to one involving only a single micelle if we neglect intermicellar interactions and the translational entropy of the micelles. The former is applicable if the micellar solution is sufficiently dilute while the latter introduces a (small) correction term to the free energy which will be included by hand later in this section. In this case, we can reduce the many-micelle system to a one-micelle system of volume V and copolymer volume fraction $\phi_{PB} + \phi_{PS}$, where V corresponds to the volume per micelle. We can then effectively vary the number density of micelles by varying V. Specifically, if the free energy of this subsystem is A, the total free energy of the macroscopic system is given by $F = (V_T/V)A$. Since V_T is fixed, we can find the equilibrium state of the whole system by minimizing the free energy density $a = A/V$ with respect to V. In the Appendix, we show using a simple two-state model that this procedure automatically yields the optimum micelle; that is, the micelle with the lowest free energy per chain.[2]

To our knowledge, this method of varying the size of the calculation box containing a single micelle in order to obtain information on a system of many micelles has not been used before: in earlier work, the box size is fixed.[29] Although having to minimize a with respect to V for each system parameter adds to the numerical burden of the calculation, the advantage of this method is that, by minimizing the free energy density, we avoid the awkward problem of trying to define the free energy per chain in the micelle, which is the basic quantity in simple theories of micellization.[2] Taking this latter approach would involve making ad hoc definitions concerning the boundary of the micelle in what is essentially a continuum calculation.

Another advantage of our approach is that it yields a well-defined value for the volume occupied by a micelle. This allows us to take into account the translational entropy of spherical micelles.[13] An estimate of the translational entropy per micelle can be obtained from a simple lattice model where the system is divided into cells of the volume of a single micelle. We adapt the results of Mayes and de la Cruz[13] and Leibler[11] and find that the translational entropy per micelle is

$$S_{trans} = -k_B \left[\ln\left(\frac{V_m}{V}\right) + \left(\frac{V - V_m}{V_m}\right) \ln\left(\frac{V - V_m}{V}\right) \right] \quad (15)$$

where V_m is the volume of the micelle and V is the volume of the subsystem containing the micelle. Note that the lattice model leading to eq 15 implicitly assumes that micelles are impenetrable. Equation 15 thus also partially corrects for intermicellar interactions which were neglected in the preceding discussion. To estimate the micelle volume, we use the working definitions of the core radius R_c and the corona thickness L_c explained in the next section; V_m can then be calculated directly from $R_c + L_c$.

We now have all the necessary techniques to calculate the optimum micelle for each system parameter. To begin, we perform an SCFT calculation at fixed subsystem volume, giving the density

profile of a micelle and the free energy density of the subsystem. We then adjust the subsystem volume. This is achieved by changing the number of points on the grid on which we solve the diffusion equations while keeping the grid step size constant. This is repeated until we have located the minimum of the free energy density for the geometry under consideration.

This procedure yields the density profile of the micelle with the minimum free energy per chain F_{chain}. As shown in the Appendix, it also results in the chemical potential of bulk copolymers outside the micelle being equal to $\min\{F_{chain}\}$. Our approach therefore also allows us to estimate the critical micelle concentration (more accurately the critical micelle volume fraction) which we define via the equation[2]

$$\phi_c - P_1 = P_1 \Rightarrow \phi_c = 2P_1 \quad (16)$$

where P_1 is the bulk copolymer concentration that coexists with the micelle at total copolymer fraction ϕ. Note that, in the original definition,[2] P_1 is the total volume fraction of copolymers that exist as isolated molecules, rather than the bulk copolymer concentration that coexists with the micelle. However, provided the micelles are well-separated, these two quantities are very close and we shall treat them as equivalent. Strictly speaking, in the above definition for ϕ_c, we should also use the bulk copolymer concentration at cmc rather than at ϕ. This is because the cmc is defined as the value of ϕ where the volume fraction of micelles equals the volume fraction of bulk copolymer. However, in practice, using the bulk copolymer fraction at ϕ rather than at cmc yields a very good approximation for ϕ_c since the bulk copolymer volume fraction remains pinned close to the cmc value for $\phi > \phi_c$. This is most readily illustrated using a simple bimodal model for micelle formation where we assume that copolymers can exist either as single molecules or as micelles with the optimum aggregation number M.[2] Denoting the micelle and single molecule fraction at ϕ as P_M and P_1, respectively, and the micelle and single molecule fraction at ϕ_c as P_{Mc} and P_{1c}, respectively, it is easy to show that for $\phi \gg \phi_c$, $P_1 = P_{1c}(\phi/\phi_c)^{1/M}$. Since M is typically large, the volume fraction of copolymers outside the micelle remains pinned close to its cmc value. For comparison with experimental data, ϕ_c is converted to weight fraction using specific volumes (eqs 1 and 2).

In the results presented in next section, the core and corona thicknesses of the spherical micelle are calculated at 10% weight fraction of copolymer, i.e., the weight fraction used in the original experiments.[5] However, the cmc values are calculated at 2.5% weight fraction of copolymer. For the copolymers with the lighter core blocks (SB 10/10, SB 40/10), the choice of weight fraction makes relatively little difference to the calculated cmc, as we would expect from the argument in the previous paragraph. However, for the copolymers with the heavier core block (SB 20/20), we need to use the dilute (2.5% weight fraction) system in order for the copolymer concentration to have reached a constant value at the edge of the system. Decreasing the copolymer weight fraction further has only a very small effect on our prediction for the cmc.

4. Results and Discussion

We begin by comparing our predictions for the core radii and corona thicknesses with experiment and scaling theory for a variety of poly(styrene−butadiene)/homopolystyrene blends. In contrast to scaling theory, the borders between the core, corona, and bulk regions are not perfectly sharp in SCFT, and we require working definitions of the core radius R_c and corona thickness L_c. We define the core radius as that at which the volume fractions of the solvophobic and solvophilic blocks are equal: $\phi_{PB}(\mathbf{r}) = \phi_{PS}(\mathbf{r})$. Other definitions, such as $\phi_{PB}(\mathbf{r}) = \phi_{PS}(\mathbf{r}) + \phi_{hPS}(\mathbf{r})$,[30] are equally valid. However, since the boundaries are quite sharp,
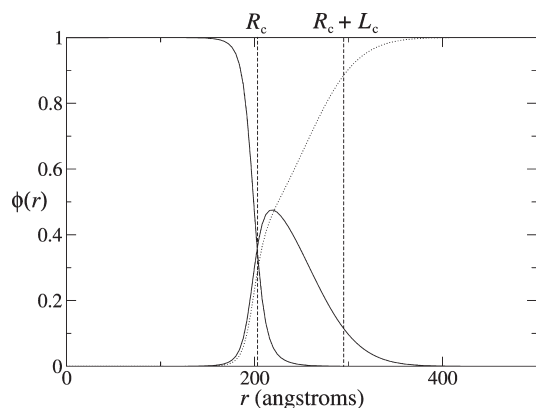
Figure 1. Cross section showing the volume fraction profiles of the various species in a spherical micelle at 115 °C as a function of the distance r from the center of the micelle. Full line: volume fraction profile for PB blocks; dashed line: PS; dotted line: homopolystyrene. The core radius R_c and the corona thickness L_c are also marked.
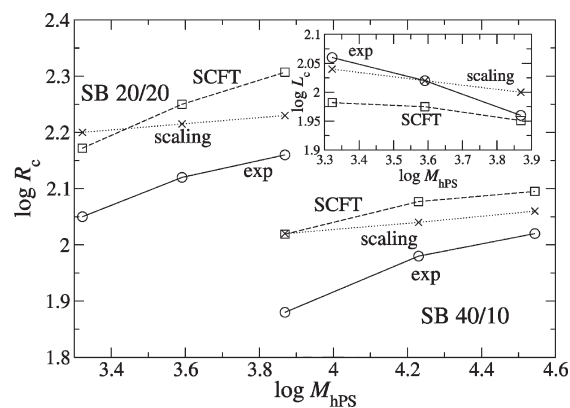

Figure 2. Main panel shows a comparison of SCFT predictions with experiment and scaling at 115 °C and copolymer weight fraction 10% for core radii R_c, as a function of homopolystyrene molecular weight. The data in the top left are for copolymers SB 20/20; those in the bottom right are for SB 40/10. The inset shows corona thickness L_c as a function of homopolystyrene molecular weight for SB 20/20. In both the main panel and the inset, solid lines with circles show experimental results, dashed lines with squares show SCFT predictions, and dotted lines with crosses show scaling.

the difference between the two definitions for a given system is quite small (see Figure 1).

In contrast, the corona is very diffuse (see Figure 1), and it is less clear how to define its outer boundary. To proceed, we calculate the radius of gyration of the corona from[31]

$$R_g^2 = \frac{\int r^2 (\phi_{PS}(r) - \phi_{PS}^b) 4\pi r^2 \, dr}{\int (\phi_{PS}(r) - \phi_{PS}^b) 4\pi r^2 \, dr} \tag{17}$$

where ϕ_{PS}^b is the bulk polystyrene concentration which must be removed to isolate the corona. We now calculate the thickness L_c of the hollow sphere with inner radius R_c (the core radius as defined above) which has the same radius of gyration as the corona. This is taken as an estimate of the corona thickness. L_c is related to R_c and R_g by[31]

$$R_g^2 = \frac{3}{5} \frac{(R_c + L_c)^5 - R_c^5}{(R_c^3 + L_c^3) - R_c^3} \tag{18}$$

and can be determined numerically.

We now examine the effect of homopolymer molecular weight on core and corona size for the samples SB 20/20 and SB 40/10.[5] The experimental data (alongside scaling theory and our SCFT predictions) are shown in Figure 2 as a plot of the logarithm of the core radius against the logarithm of the homopolymer molecular weight. As the homopolystyrene molecular weight is decreased at a fixed polystyrene block molecular weight, we see that the corona thickness increases and the core radius decreases. This is because decreasing homopolystyrene length leads the entropy of mixing between the homopolystyrene and the polystyrene block to increase, increasing the tendency of the homopolystyrene volume fraction profile to be uniform. This can be achieved by making the corona region larger and the core smaller.[5] These data also show the effect of core block molecular weight: if a copolymer with a larger PB block (SB 20/20 rather than SB 40/10) is used, the core radius is naturally larger.

The shape of these experimentally observed trends are reproduced much more accurately by SCFT (see Figure 2) compared to scaling theory, where the predicted variation of R_c with M_{hPS} is too shallow. On the other hand, for both SB 20/20 and SB 40/10, SCFT overestimates R_c by about 20–30%; this discrepancy is comparable to that found in scaling theory. However, we emphasize that our calculations contain no adjustable parameters: all the required input concerning polymer properties (such as the interaction density Λ) has been determined from

experiments that do not involve micelle formation. Given this fact, we believe that the agreement between SCFT and experiment for R_c is good.

With our corona definition, SCFT reproduces the experimentally observed fall in corona thickness as the homopolymer molecular weight is increased for the sample SB 20/20 (see inset to Figure 2). However, both SCFT and scaling theory predict a variation of L_c with M_{hPS} that is too shallow. In terms of the magnitude of L_c, scaling theory is marginally more accurate compared to SCFT, though the difference between either SCFT or scaling theory with experiment is small. We also note that the corona is very diffuse, and its radius is measured in experiments by an indirect procedure (it is inferred from the interparticle interactions).[32] The measurements of the corona thickness do not therefore constitute as stringent a test of the theory as those of the core radius.

In terms of the variation of R_c or L_c with M_{hPS}, experimental data are available for heavier copolymers (SB 80/80).[5] Unfortunately, we have not been able to test SCFT for this system because χN is too high and the core density profile too sharp so that our extremization procedure becomes unreliable due to numerical errors.

Next, we consider the dependence of the core radius on the polystyrene block molecular weight (rather than the homopolystyrene weight considered above). As before, the SCFT predictions, scaling theory and experimental data are shown in a log–log plot (Figure 3). The PB block molar weight is fixed at ~10 kg/mol, while the PS block molar weight is increased from around 10 kg/mol to 60 kg/mol. The homopolymer is always 7400PS. From the experimental data, the PB core is seen to shrink as the PS block molecular weight is increased. This behavior can be understood (see the explanation given above) by considering the effect of the polystyrene molecular block weight (this time at fixed homopolystyrene weight) on the entropy of mixing outside the core.[5]

For the SCFT curve labeled "SCFT", the PB block molar weight for each copolymer sample is fixed at the value quoted in the original paper;[5] i.e., the copolymer samples considered in Figure 3 do not all have the same PB block molar weight, but instead have a range of molar weights in the region of 10 kg/mol. In this case, SCFT does not predict the shape of R_c vs M_{PS} very well. In particular, the predicted R_c is no longer a monotonically decreasing function of M_{PS}. The scatter in the SCFT points
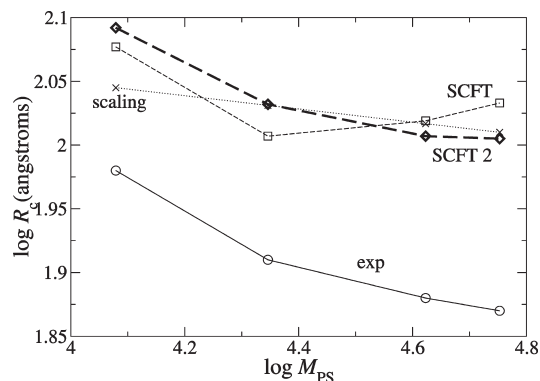
Figure 3. Comparison of SCFT predictions (dashed lines with squares) with experiment (solid lines with circles) and scaling (dotted lines with crosses) at 115 °C and 10% copolymer weight fraction for core radii R_c, as a function of polystyrene block molecular weight. The molecular weight of the polybutadiene (core) block is held approximately constant. The line labeled SCFT uses the core block molecular weights used in the experiment; the bolder line labeled SCFT2 fixes the core block molecular weight at 10 kg/mol. See the text for a discussion.
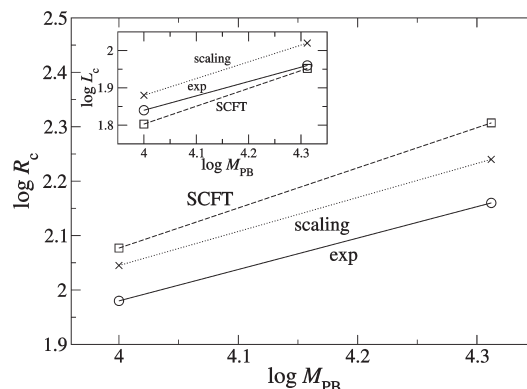

Figure 4. Comparison of SCFT predictions (dashed lines with squares) with experiment (solid lines with circles) and scaling (dotted lines with crosses) at 115 °C, as a function of polybutadiene block molecular weight for symmetric copolymers. Main panel shows core radii R_c; inset shows corona thickness L_c. The homopolystyrene molecular weight is fixed at 7400 g/mol.

comes from the fact that within SCFT R_c is very sensitive to the exact molecular weight of the core block so any scatter in the input PB block weight is amplified in the final R_c results. In particular, the sample SB 23/10 (the second point in Figure 3) has the rather lower value of 9 kg/mol, which leads to an apparent minima in the R_c values.

If, on the other hand, we fix the core block for all the samples to be 10 kg/mol, we obtain the curve labeled "SCFT2", which now predicts the shape of R_c vs M_{PS} much more accurately. In fact, fixing the PB block weight of all the samples to be 10 kg/mol lies well within the experimental accuracy of the measured molecular weights since the polydispersity for all the copolymer samples can be as high as $M_w/M_n = 1.05$,[32] which translates to an uncertainty in the molecular weight of $\langle \Delta M^2 \rangle^{1/2}/M_n \approx 20\%$ (recall[33] that $\langle \Delta M^2 \rangle^{1/2}/M_n = M_w/M_n - 1$). We note that the curve SCFT2 predicts the shape of R_c vs M_{PS} much more accurately than scaling theory, where the predicted variation of R_c with M_{PS} is too shallow. However, as before, SCFT overestimates R_c by about 30%, similar to scaling theory.

We now move to the dependence of the core radius and corona thickness on the overall copolymer molecular weight for *symmetric* copolymers. We consider the samples SB 10/10 and SB 20/20 in 7400PS homopolymer and, as before, show experimental, scaling,[5] and SCFT results in a log–log plot (Figure 4). As would be expected, the core radius and corona thickness both increase as the molecular weight of the symmetric diblocks is increased. For the available points, both SCFT and scaling theory predict the slope of R_c vs M_{PB} well. However, both theories once again overestimate the magnitude of R_c, though scaling theory is marginally more accurate than SCFT in this case. The situation is reversed for the corona thickness (inset of Figure 4) where SCFT is marginally more accurate than scaling theory. Unfortunately, we are unable to confirm whether these trends continue to higher copolymer weights because although experimental data are available for heavier copolymers,[5] we encounter numerical difficulties in modeling these because of the high χN values involved.

Our final comparison of SCFT with experiment and scaling theory focuses on the data of Kinning et al. concerning the cmc. These show that the cmc decreases with increasing copolymer molecular weight (at fixed copolymer composition) and with increasing homopolystyrene molecular weight. It also increases with increasing polystyrene block length (see Figure 5). These broad trends are successfully reproduced by scaling theory[11] (see Figure 5). However, the scaling theory
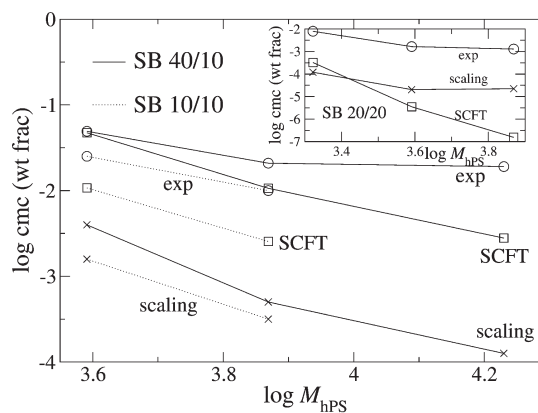

Figure 5. Comparison of SCFT predictions (squares) with experiment (circles) and scaling (crosses) for the critical micelle concentration at 115 °C, as a function of homopolystyrene molecular weight. Main panel: solid lines show data for copolymers SB 40/10; dotted lines show results for copolymers SB 10/10. Inset: data for copolymers SB 20/20.

cmcs are 1−2 orders of magnitude smaller than those measured.[5]

We find (see Figure 5) that SCFT also successfully reproduces the general trends outlined above. Furthermore, for copolymers with short polybutadiene blocks (SB 10/10 and SB 40/10), SCFT predictions improve on those of scaling theory by around an order of magnitude, although the cmc is still underestimated. However, for the copolymer sample with the longest solvophobic block (SB 20/20), the SCFT values for the cmc are very low and are in fact inferior to those predicted by scaling theory (see inset to Figure 5). Interestingly, similar results were found by Wijmans and Linse.[34] They compared SCFT with Monte Carlo simulations for a system of AB diblock copolymers in A monomer solvent, and the cmc predicted by SCFT was found to be much lower than that measured in the simulations (see also the similar comparison in the simulation and SCFT work of Cavallo et al.)[28]. Wijmans and Linse argued that this was due to the effect of the mean-field approximation on the bulk chemical potential. The argument is as follows.[34] In mean-field theory, the effect of compositional fluctuations where an individual copolymer interacts with itself are neglected, so that a copolymer in the bulk region interacts almost exclusively with the solvent. The solvophobic B section of the copolymer therefore interacts largely with the A solvent, and the number of repulsive contacts is very high. However, in Monte Carlo simulations or experiment, the B block
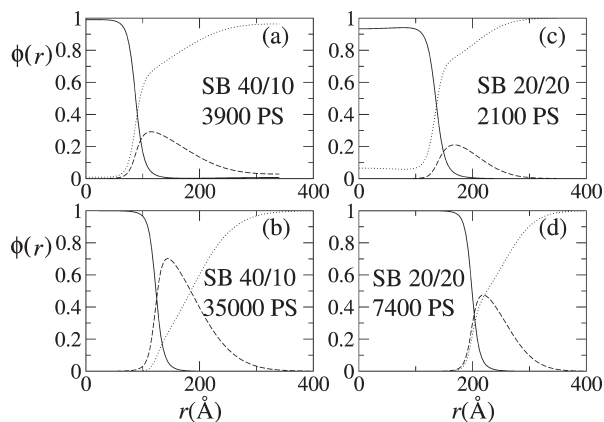
Figure 6. All panels show cuts through the volume fraction profiles for micelles. The core PB blocks are shown by full lines, the corona PS blocks by dashed lines, and the polystyrene homopolymer by dotted lines. Panel (a) shows the profiles for the asymmetric copolymer SB 40/10 blended with the light homopolymer 3900 PS. Panel (b) shows the corresponding plots for the same copolymer blended with the very heavy homopolymer 35000 PS. The decreased mixing of the homopolymer with the corona and corresponding swelling of the core as the homopolymer molecular weight is increased may clearly be seen. Panel (c) shows volume fraction profiles for the strongly solvophobic, symmetric copolymer SB 20/20 in the light homopolymer 2100 PS, while panel (d) shows the corresponding plots in the heavier 7400 PS. As in panels (a) and (b), the difference in core size and corona swelling between the two blends may be clearly seen. In addition, the very light homopolymer 2100 PS mixes significantly with the core PB blocks in panel (c).

minimizes contact with the solvent by collapsing into a globule, so that the number of repulsive interactions is smaller than that predicted by mean-field theory. This means that the bulk phase is more energetically unfavorable in SCFT, and micelle formation is hence more favorable in comparison. The cmc is therefore underestimated by SCFT. If the above argument is correct, we would expect the disagreement to worsen sharply when we consider polymers with longer solvophobic blocks. This is indeed seen for SB 20/20.

Interestingly, the agreement between scaling theory and experiment for SB 20/20 is not as bad, despite the fact that a mean field Flory−Huggins model is employed for the bulk free energy[11] (see the inset to Figure 5). We speculate that the better agreement may be due to a fortuitous cancellation of errors due to the approximate nature of the free energy used in scaling theory for both the micelle and the bulk. In contrast, we expect the SCFT free energy to be very accurate for the micelle (as evidenced by the excellent agreement of core dimensions) but significantly poorer for the bulk for the reasons explained in the previous paragraph.

By plotting density profiles of the micelles for the SB 20/20 and SB 40/10 samples blended with the heaviest and lightest homopolymers considered in the experiments, we may clearly demonstrate the swelling of the core and corresponding shrinking of the corona as the homopolymer weight is increased. All profiles are calculated at 10% weight fraction. In panel (a) of Figure 6, we show cuts through the density profile of the optimum micelle formed by SB 40/10 in 3900 PS for the various species. The volume fraction profiles of the core PB blocks, corona PS blocks, and homopolystyrene are shown by full lines, dashed lines, and dotted lines, respectively. For this system, the small homopolymer has a high entropy of mixing with the polystyrene corona. This means that the corona is strongly swollen by the homopolymer, and the core shrinks to compensate.[5,35] The opposite extreme may be seen in panel (b) of Figure 6, where cuts are shown through the volume fraction profile of a micelle in a blend of SB 40/10 copolymer with the heavy homopolymer 35000PS.

Here, the large homopolystyrene molecules mix much less well with the corona PS blocks, and the volume fraction of homopolymer in the corona region is much lower. This results in a clear increase of the core radius from around 95 Å to around 125 Å.

In the second pair of panels (c and d) in Figure 6, we consider the symmetric and more strongly solvophobic copolymer SB 20/20. Again, a decrease in the swelling of the corona by homopolymer and an increase in the core radius are seen as the sample is blended with heavier homopolystyrene molecules. In addition, panel (c) shows clear penetration of the very light homopolymer 2100 PS into the micelle core.

5. Conclusions

We have found that self-consistent field theory gives a good description of all the experimentally measured trends of spherical micelle structure. In particular, we find that SCFT reproduces the shape of the variation of R_c with different molecular parameters much more accurately compared to scaling theory, though, like scaling theory, it overestimates R_c by about 20−30%. We note however that our calculations contain no adjustable parameters. Given this fact, we believe that the agreement between SCFT and experiment for R_c is good. Since the core radius is the quantity most accurately measured experimentally, the success of SCFT here is clear validation of the use of this approach to model micelle formation in block copolymer/homopolymer blends. For the corona thickness L_c, we find that the accuracy of our SCFT results is at least as good as those of scaling theory. However, we note that this quantity is measured indirectly[32] and is subject to larger experimental error.

SCFT predicts the qualitative trends for the cmc as the homopolymer molecular weight and copolymer composition and molecular weight are varied. For smaller core block molecular weights, the predictions improve on scaling theory by around an order of magnitude. For heavier core blocks, the agreement between SCFT and experiment worsens. This problem was attributed to the overestimation by SCFT of the energy difference between a copolymer in the micelle and one in the bulk.[34]

In summary, we have shown that SCFT provides a very good description of micelle structure and hence that it is a suitable tool for studying the micellization in block copolymer systems. It is less successful in predicting absolute values of the cmc, although the correct qualitative trends are obtained. This is characteristic of a mean-field approximation to a many-body theory: for example, the mode-coupling theory of the glass transition[36] successfully describes the strength of arrest on different length scales within a structural glass but is less effective in predicting the temperature at which this effect occurs.[36]

Appendix. Simple Two-State Model for Micelle Formation

Consider a copolymer solution with volume V and copolymer volume fraction ϕ containing a single micelle. To simplify our calculation, we assume a simple two-state model for this system where there is a sharp demarcation between micelle and bulk so that copolymer chains can exist either in the micelle or in the bulk and let the number of copolymer chains in the micelle and bulk be n and m, respectively. The free energy of this single micelle system is then given by[2]

$$A = nf(n) + mk_BT\left(\ln\frac{m}{V} - 1\right) + mf(1) \quad (19)$$

where $f(n)$ is the energy per chain for a micelle with aggregation number n arising from contributions other than the translational

entropy of the copolymer chains. The first term on the right-hand side of eq 19 is the contribution to the free energy from copolymers in the micelle (neglecting the translational entropy of the micelle) while the second and third terms are due to translational entropy and nontranslational entropy contributions, respectively, of copolymers in the bulk. We now assume that V is the volume per micelle in a many micelle system with total volume V_T and copolymer volume fraction ϕ. If we neglect the translational entropy of micelles, intermicellar interactions, and micelle polydispersity, the total free energy of the many micelle system is given by

$$F = \frac{V_T}{V} A \qquad (20)$$

To find the equilibrium state of the system, we need to minimize F with respect to n, m, and V (the internal degrees of freedom of the system) subject to the constraint that the total number of copolymer chains is fixed, i.e.

$$\frac{V_T}{V}(m+n) = \frac{V_T \phi}{V_0} \qquad (21)$$

where V_0 is the volume per copolymer chain. This is equivalent to minimizing the modified free energy

$$F_\mu = \frac{V_T}{V} A - \mu \frac{V_T}{V}(m+n) \qquad (22)$$

with respect to m, n, and V where μ is a Lagrange multiplier imposing the mass conservation constraint eq 21.

From $\partial F_\mu / \partial n = 0$, we find

$$\frac{\partial A}{\partial n} = f(n) + n f'(n) = \mu \qquad (23)$$

where $f'(n)$ is the derivative of $f(n)$ with respect to n. From $\partial F_\mu / \partial m = 0$ we find

$$\frac{\partial A}{\partial m} = k_B T \ln \frac{m}{V} + f(1) = \mu \qquad (24)$$

Equations 23 and 24 allow us to identify μ as the chemical potential of copolymer chains in the micelle and the bulk, respectively, and also tell us that at equilibrium the two chemical potentials are equal.

From $\partial F_\mu / \partial V = 0$ we find

$$A - \mu(m+n) + m k_B T = 0 \qquad (25)$$

Using eqs 19 and 24, the above equation simplifies to

$$f(n) = \mu \qquad (26)$$

Finally, inserting eq 26 into eq 23, we find

$$f'(n) = 0 \qquad (27)$$

Thus, minimizing F_μ with respect to n, m, and V yields the equilibrium condition for micellization condition to be that the free energy per chain in the micelle is minimized (eq 27) and the chemical potential of copolymer chains in the system is equal to the minimized free energy per chain (eq 26). These results agree with the equilibration condition derived from simple theories for micellization,[2] thus validating the approach used in this paper.

References and Notes

(1) Jain, S.; Bates, F. S. *Science* **2003**, *300*, 460–464.
(2) Safran, S. A. *Statistical Thermodynamics of Surfaces, Interfaces, and Membranes*; Westview Press: Boulder, 1994.
(3) Zhulina, E. B.; Adam, M.; LaRue, I.; Sheiko, S. S.; Rubinstein, M. *Macromolecules* **2005**, *38*, 5330–5351.
(4) Kim, Y.; Dalhaimer, P.; Christian, D. A.; Discher, D. E. *Nanotechnology* **2005**, *16*, S484–S491.
(5) Kinning, D. J.; Thomas, E. L.; Fetters, L. J. *Macromolecules* **1991**, *24*, 3893–3900.
(6) Roe, R.-J. *Macromolecules* **1986**, *19*, 728–731.
(7) Matsen, M. W. In *Soft Matter*; Wiley-VCH: Weinheim, 2006; Chapter 2.
(8) *Polymer Handbook*; Brandrup, J., Immergut, E. H., Eds.; Wiley: New York, 1989.
(9) Rigby, D.; Roe, R.-J. *Macromolecules* **1984**, *17*, 1778–1785.
(10) Rigby, D.; Roe, R.-J. *Macromolecules* **1986**, *19*, 721–728.
(11) Leibler, L.; Orland, H.; Wheeler, J. C. *J. Chem. Phys.* **1983**, *79*, 3550–3557.
(12) Whitmore, M. D.; Noolandi, J. *Macromolecules* **1985**, *18*, 657–665.
(13) Mayes, A. M.; de la Cruz, M. O. *Macromolecules* **1988**, *21*, 2543–2547.
(14) Edwards, S. F. *Proc. Phys. Soc.* **1965**, *85*, 613–624.
(15) Leermakers, F. A. M.; Wijmans, C. M.; Fleer, G. J. *Macromolecules* **1995**, *28*, 3434–3443.
(16) Leermakers, F. A. M.; Scheutjens, J. M. H. M. *J. Colloid Interface Sci.* **1990**, *136*, 231–241.
(17) Linse, P. *Macromolecules* **1993**, *26*, 4437–4449.
(18) Wang, J.; Wang, Z. G.; Yang, Y. *Macromolecules* **2005**, *38*, 1979–1988.
(19) Duque, D. *J. Chem. Phys.* **2003**, *119*, 5701–5704.
(20) Monzen, M.; Kawakatsu, T.; Doi, M.; Hasegawa, R. *Comput. Theor. Polym. Sci.* **2000**, *10*, 275–280.
(21) Richardson, M. J.; Savill, N. G. *Polymer* **1977**, *18*, 3–9.
(22) Roe, R.-J.; Zin, W.-C. *Macromolecules* **1980**, *13*, 1221–1228.
(23) Jones, R. A. L. *Soft Condensed Matter*; Oxford University Press: Oxford, 2002.
(24) Fredrickson, G. H. *The Equilibrium Theory of Inhomogeneous Polymers*; Oxford University Press: Oxford, 2006.
(25) Bates, F. S.; Fredrickson, G. H. *Annu. Rev. Phys. Chem.* **1990**, *41*, 525–57.
(26) Matsen, M. W. *J. Chem. Phys.* **2004**, *121*, 1938–1948.
(27) Press, W. H.; Flannery, B. P.; Teukolsky, S. A.; Vetterling, W. T. *Numerical Recipes in C*, 2nd ed.; Cambridge University Press: Cambridge, 1992.
(28) Cavallo, A.; Müller, M.; Binder, K. *Macromolecules* **2006**, *39*, 9539–9550.
(29) van Lent, B.; Scheutjens, J. M. H. M. *Macromolecules* **1989**, *22*, 1931–1937.
(30) Katsov, K.; Müller, M.; Schick, M. *Biophys. J.* **2004**, *87*, 3277–3290.
(31) Burchard, W. *Adv. Polym. Sci.* **1983**, *48*, 1–124.
(32) Kinning, D. J.; Thomas, E. L.; Fetters, L. J. *J. Chem. Phys.* **1989**, *90*, 5806–5825.
(33) Strobl, G. *The Physics of Polymers*; Springer-Verlag: Berlin, 1996.
(34) Wijmans, C. M.; Linse, P. *Langmuir* **1995**, *11*, 3748–3756.
(35) Kinning, D. J.; Winey, K. I.; Thomas, E. L. *Macromolecules* **1988**, *21*, 3502–3506.
(36) Götze, W. *J. Phys.: Condens. Matter* **1999**, *11*, A1–A45.